Supplementary Information

Synthesis, structure, and properties of twisted π-conjugated molecules featuring three-dimensional π-π interactions in solid states

Mai Nagase,[a,b] Ryu Yoshida,[a,b] Sachiko Nakano,[a] Takashi Hirose[c] and Yasutomo Segawa*[a,b]

[a] *Institute for Molecular Science, Myodaiji, Okazaki, 444-8787, Japan*
[b] *The Graduate University for Advanced Studies, SOKENDAI, Myodaiji, Okazaki, 444-8787, Japan*
[c] *Institute for Chemical Research, Kyoto University, Uji, Kyoto, 611-0011, Japan*

E-mail: segawa@ims.ac.jp

Table of Contents

1. Experimental section

General

Unless otherwise noted, all materials were obtained from commercial suppliers and used without further purification. Tetrahydrofuran (THF) and toluene for reactions were purified by passing through a solvent purification system (Glass Contour). All reactions were performed with dry solvents under an atmosphere of nitrogen in dried glassware with standard vacuum-line techniques. Work-up and purification procedures were carried out with reagent-grade solvents under air. Tetra(3,4-thienylene) (**3**)[S1] and **4**[S2] were synthesized according to reported procedure.

Analytical thin-layer chromatography (TLC) was performed using E. Merck silica gel 60 F254 precoated plates (0.25 mm). The developed chromatograms were analyzed by UV lamp (254 or 365 nm). Silica gel column chromatography was performed with KANTO Silica Gel 60N (spherical, neutral, 40-100 μm) or Biotage Isolera® equipped with Biotage® Sfär Silica D Duo 60 μm columns. Preparative recycling gel permeation chromatography (GPC) was performed with a YMC LC-forte/R instrument equipped with JAIGEL-1HH (20 mm I.D. × 600 mm) and JAIGEL-2HH columns (20 mm I.D. × 600 mm) using chloroform ($CHCl_3$) as an eluent. The high-resolution mass spectra (HRMS) were obtained from a JEOL JMS-T100GC AccuTOFTM GC-TOFMS equipped with Agilent 6890N GC. Melting points were measured on a MPA100 Optimelt automated melting point system. Nuclear magnetic resonance (NMR) spectra were recorded on a JEOL JNM-ECS400 (^1H 400 MHz, ^{13}C 100 MHz) spectrometer. Chemical shifts for ^1H NMR are expressed in parts per million (ppm) relative to $CHCl_3$ (δ 7.26 ppm). Chemical shifts for ^{13}C NMR are expressed in ppm relative to $CDCl_3$ (δ 77.16 ppm). Data are reported as follows: chemical shift, multiplicity (s = singlet, d = doublet), coupling constant (Hz), and integration.

Synthesis of 1

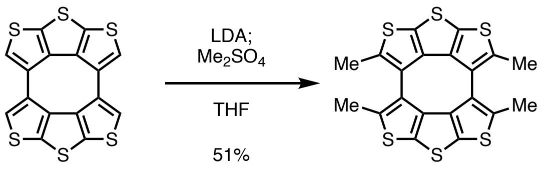

4 **1**

To a 100-mL two-necked flask containing a magnetic stirring bar was added **4** (200 mg, 515 µmol, 1.0 equiv.). The flask was evacuated and backfilled with nitrogen three times, and THF (200 mL) was added. The hexane/THF solution of lithium diisopropylamide (LDA; 1.1 M, 9.4 mL, 10.3 mmol, 20 equiv.) was added at 0 °C and the reaction mixture was stirred at 0 °C for 2 h. Dimethyl sulfate (0.98 mL, 10.3 mmol, 20 equiv.) was added at 0 °C and the reaction mixture was stirred at room temperature for 18 h. The reaction mixture was quenched with water, extracted with chloroform, washed with brine, dried over Na_2SO_4, and then evaporated *in vacuo*. The crude product was purified by silica gel column chromatography (eluent: dichloromethane) and GPC (eluent: chloroform) to afford **1** as a yellow solid (118 mg, 51%).

^{1}H NMR (400 MHz, $CDCl_3$): δ 2.49 (s, 12H); ^{13}C NMR (100 MHz, $CDCl_3$): δ 137.6 (4°), 136.7 (4°), 133.9 (4°), 126.0 (4°), 18.4 (CH_3); HRMS (GC EI-TOF MS) *m/z* calcd for $C_{20}H_{12}S_4$ $[M]^+$: 443.9258, found: 443.9264; mp: >250 °C.

Synthesis of 5

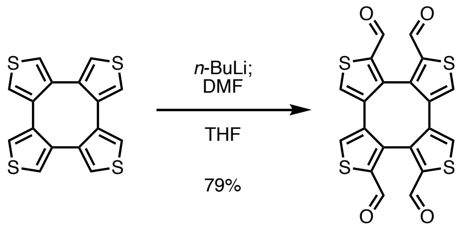

3 5

To a 200-mL two-necked flask containing a magnetic stirring bar was added **3** (1.49 g, 4.54 mmol). The flask was evacuated and backfilled with nitrogen three times, and THF (75 mL) was added. The hexane solution of ^{n}BuLi (2.66 M, 7.70 mL, 20.0 mmol, 4.5 equiv.) was added at –78 °C and the reaction mixture was stirred at room temperature for 2 h. *N*,*N*-Dimethylformamide (DMF; 2.8 mL, 36.3 mmol, 8 equiv.) was added at –78 °C and the reaction mixture was stirred at room temperature for 18 h. The reaction mixture was quenched with water, extracted with EtOAc, washed with brine, dried over Na$_2$SO$_4$, and then evaporated *in vacuo*. The crude product was purified by silica gel column chromatography (eluent: hexane/EtOAc = 50:50 to 20:80) to afford **5** as a yellow solid (1.58 g, 79%).

^{1}H NMR (400 MHz, CDCl$_3$): δ 9.623 (s, 2H), 9.620 (s, 2H), 7.788 (s, 2H), 7.785 (s, 2H); ^{13}C NMR (100 MHz, CDCl$_3$): δ 182.4 (CH), 143.8 (4°), 138.9 (4°), 137.2 (4°), 134.0 (CH); HRMS (GC EI-TOF MS) *m/z* calcd for C$_{20}$H$_8$O$_4$S$_4$ [M]$^+$: 439.9300, found: 439.9296; mp: >250 °C.

Synthesis of 6

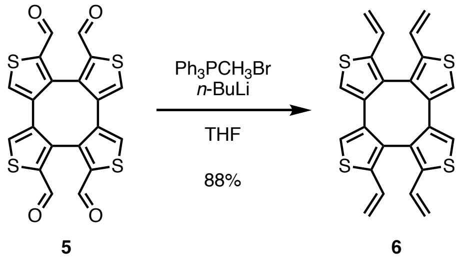

To a 500-mL two-necked flask containing a magnetic stirring bar was added Ph_3PCH_3Br (5.65 g, 15.8 mmol, 4.4 equiv.). The flask was evacuated and backfilled with nitrogen three times, and THF (80 mL) was added. The hexane solution of ^{n}BuLi (2.66 M, 5.95 mL, 15.8 mmol, 4.4 equiv.) was added at –10 °C and the reaction mixture was stirred at room temperature for 30 min. The THF (140 mL) solution of **5** (1.58 g, 3.60 mmol) was added to the flask and the reaction mixture was stirred at room temperature for 18 h. The reaction mixture was quenched with saturated NH_4Cl aqueous solution, extracted with chloroform, washed with brine, dried over Na_2SO_4, and then evaporated *in vacuo*. The crude product was purified by silica gel column chromatography (eluent: hexane/EtOAc = 90:10 to 70:30) to afford **6** as a yellow solid (1.37 g, 88%).

^{1}H NMR (400 MHz, $CDCl_3$): δ 7.02 (s, 4H), 6.42 (dd, *J* = 17.2, 11.2 Hz), 5.55 (d, *J* = 17.2 Hz), 5.08 (d, *J* = 11.2 Hz); ^{13}C NMR (100 MHz, $CDCl_3$): δ 140.8 (4°), 138.6 (4°), 133.1 (4°), 129.8 (CH), 121.6 (CH), 114.0 (CH_2); The mass signal was not detected; mp: 99–105 °C (decomposed).

Synthesis of 7

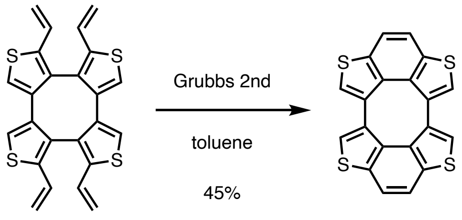

6 **7**

To a 50-mL two-necked flask containing a magnetic stirring bar were added **6** (113 mg, 300 μmol, 1.0 equiv.) and Grubbs 2nd catalyst (25.6 mg, 30.0 μmol, 10 mol%). The flask was evacuated and backfilled with nitrogen three times, and toluene (20 mL) was added. The reaction mixture was stirred at reflux for 18 h. The reaction mixture was evaporated *in vacuo* and purified by silica gel column chromatography (eluent: hexane/EtOAc = 80:20) to afford **7** as a brown solid (44.4 mg, 45%).

^{1}H NMR (400 MHz, $CDCl_3$): δ 7.85 (s, 4H), 7.58 (s, 4H); ^{13}C NMR (100 MHz, $CDCl_3$): δ 138.4 (4°), 134.1 (4°), 130.9 (4°), 127.1 (CH), 119.7 (CH); HRMS (GC EI-TOF MS) *m/z* calcd for $C_{20}H_8S_4$ $[M]^+$: 375.9503, found: 375.9485; mp: 189–194 °C (decomposed).

Synthesis of 2

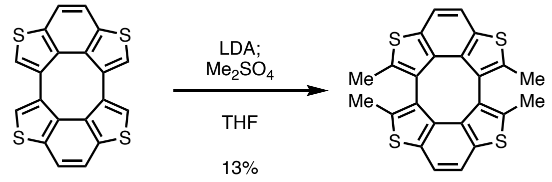

7 **2**

To a 100-mL two-necked flask containing a magnetic stirring bar was added **7** (58.3 mg, 155 µmol, 1.0 equiv.). The flask was evacuated and backfilled with nitrogen three times, and THF (23 mL) was added. The hexane/THF solution of LDA (1.1 M, 2.8 mL, 3.1 mmol, 20 equiv.) was added at 0 °C and the reaction mixture was stirred at 0 °C for 2 h. Dimethyl sulfate (0.44 mL, 4.7 mmol, 30 equiv.) was added at 0 °C and the reaction mixture was stirred at room temperature for 18 h. The reaction mixture was quenched with methanol, extracted with chloroform, washed with brine, dried over Na_2SO_4, and then evaporated *in vacuo*. The crude product was purified by silica gel column chromatography (eluent: hexane/EtOAc = 90:10) and GPC (eluent: chloroform) to afford **2** as a yellow solid (9.0 mg, 13%).

^{1}H NMR (400 MHz, $CDCl_3$): δ 7.63 (s, 4H), 2.28 (s, 12H); ^{13}C NMR (100 MHz, $CDCl_3$): δ 140.6 (4°), 134.0 (4°), 133.1 (4°), 128.6 (4°), 117.9 (CH), 16.5 (CH_3); HRMS (GC EI-TOF MS) *m/z* calcd for $C_{24}H_{16}S_4$ $[M]^+$: 432.0129, found: 432.0140; mp: 155–160 °C (decomposed).

2. X-ray crystallography

Details of the crystal data and a summary of the intensity data collection parameters for **7**, **1**, and **2** are listed in Table S2. Suitable crystals were mounted with mineral oil on a MiTeGen MicroMounts and transferred to the kappa goniometer of a RIGAKU XtaLAB Synergy Custom system equipped with mirror monochromated Mo Kα radiation (λ = 0.71073 Å) and HyPix-6000HEIC detector. Cell parameters were determined and refined, and raw frame data were integrated using CrysAlisPro (Rigaku Oxford Diffraction, 2018). The structures were solved by dual methods using SHELXT[S4] and refined by full-matrix least-squares techniques against F^2 with SHELXL-2018/3[S5] using Olex2 software package.[S6] The intensities were corrected for Lorentz and polarization effects. All non-hydrogen atoms were refined with anisotropic displacement parameters. Hydrogen atoms were placed using AFIX instructions and refined isotropically.

Table S2. Crystallographic data and structure refinement details of **7**, **1**, and **2**.

	7	**1**	**2**
CCDC No.	2417361	2417362	2417363
formula	$C_{10}H_4S_2$	$C_{20}H_{12}S_6$	$C_{24}H_{16}S_4$
fw	188.25	444.66	432.61
T (K)	143(2)	143(2)	143(2)
λ (Å)	0.71073	0.71073	0.71073
cryst syst	monoclinic	monoclinic	monoclinic
space group	$C2/c$	$I2/a$	$P2/n$
a (Å)	13.0360(7)	13.9881(3)	12.0579(5)
b (Å)	9.2577(4)	11.6422(3)	7.6145(3)
c (Å)	12.7472(7)	22.2132(5)	21.3949(7)
α (deg)	90	90	90
β (deg)	105.591(6)	92.097(2)	105.709(4)
γ (deg)	90	90	90
V (Å^3)	1481.77(14)	3615.05(15)	1891.00(13)
Z	8	8	4
D_{calc} (g·cm^{-3})	1.688	1.634	1.520
μ (mm^{-1})	0.638	0.759	0.511
F(000)	768.0	1824.0	896.0
cryst size (mm)	0.10 × 0.08 × 0.01	0.15 × 0.15 × 0.15	0.05 × 0.05 × 0.05
2θ range (deg)	5.468–62.818	5.782–59.486	5.35–59.16
reflns collected	5646	14624	16448
indep reflns/R_{int}	2006 / 0.0269	4149 / 0.0230	4323 / 0.0359
params	109	239	257
GOF on F^2	1.072	1.051	1.118
R_1, wR_2 [$I>2\sigma(I)$]	0.0336, 0.0864	0.0268, 0.0678	0.0843, 0.2003
R_1, wR_2 (all data)	0.0420, 0.0900	0.0309, 0.0702	0.1060, 0.2093

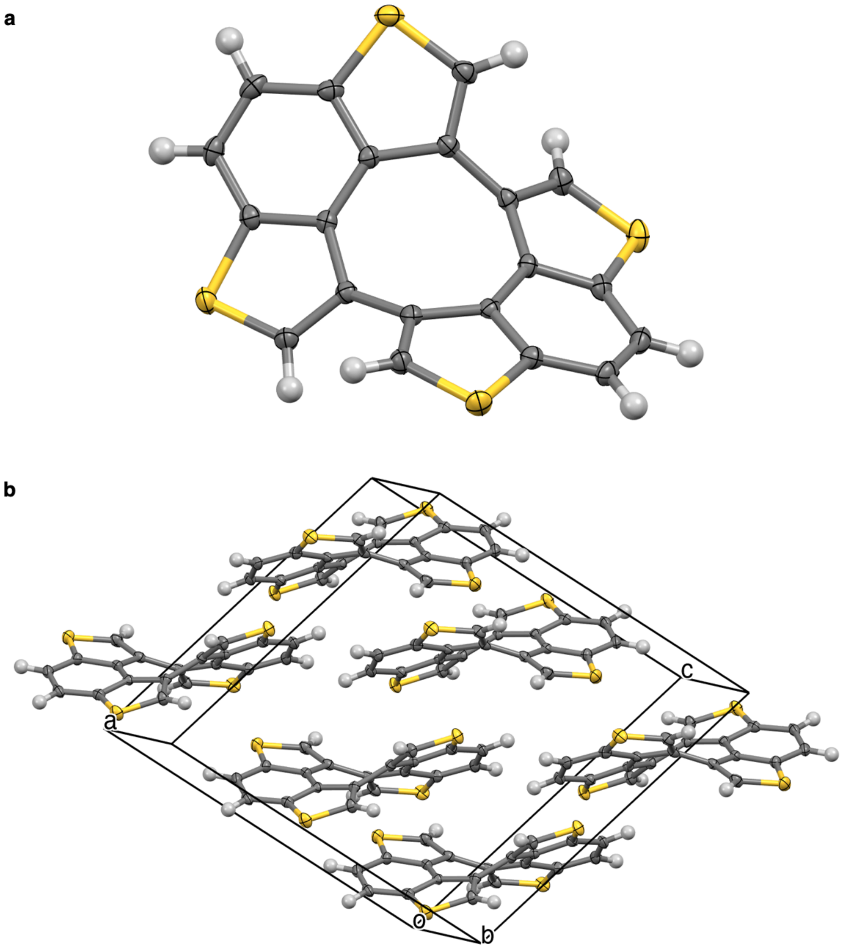

Fig. S1 (a) The X-ray crystal structure of **7** with thermal ellipsoids at 50% probability. (b) Packing mode of **7**.

3. Photophysical measurement

UV-vis absorption spectra were recorded on a JASCO V-770 spectrometer with a resolution of 0.5 nm. Fluorescence spectra were recorded on a JASCO FP-8600 spectrometer. Dilute solutions in spectral-grade degassed dichloromethane in a 1 cm square quartz cell were used for measurements. Absolute fluorescence quantum yields were determined by a Hamamatsu Photonics Quantaurus-QY® absolute PL quantum yield spectrometer C11347-01. Fluorescence lifetime were measured by a Hamamatsu Photonics Quantaurus-Tau® fluorescence lifetime spectrometer C11367-21 with LED as a light source.

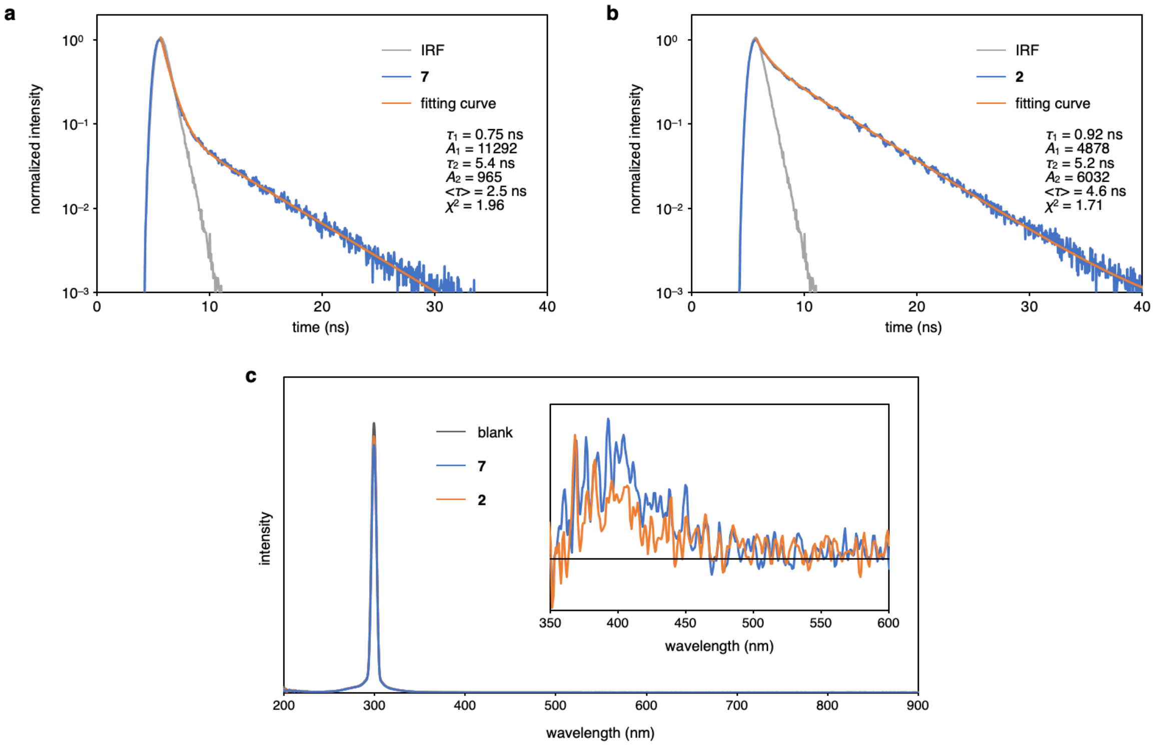

Fig. S2 (a and b) The instrument response function (IRF) and fluorescence decay curves of **7** (a) and **2** (b) monitored at 400 nm following excitation at 340 nm with the fitting curves using bi-exponential decay functions; averaged lifetime $<\tau> = (A_1\tau_1^2 + A_2\tau_2^2)/(A_1\tau_1 + A_2\tau_2)$ where A_n are amplitudes of τ_n. (c) Spectra for the determination of absolute fluorescence quantum yields of **2** and **7** upon excitation at 300 nm where magnified spectra were shown in the inset.

4. Fabrication and evaluation of OFETs

All OFET devices were fabricated in a bottom-contact, bottom-gate configuration on heavily doped n-type Si(100) wafers (0.001–0.002 Ω cm) with a 200 nm-thick SiO_2 dielectric layer. The 40 nm thickness of gold was vacuum-deposited on top of the surface through a shadow mask to define the source and drain electrodes. The channel length (L) and channel width (W) were 50 and 1500 μm, respectively. The substrates were subjected to surface modification with hexamethyldisilazane (HMDS) and pentafluorothiophenol (PFBT) or not modified. On the substrates, 40 nm thickness of **1** was thermally evaporated under vacuum with the deposition rates of 0.2 Å s^{-1}. The transfer and output characteristics of the fabricated OFET devices were measured using a B2902A source measure unit (Keysight Technologies) in a nitrogen-filled glove box. Field-effect mobilities (μ) were determined from the transfer curves in the saturation regime of the drain current (I_D), using the following equation:

$$I_D = (W/2L)\mu C_i(V_G - V_{th})^2$$

where C_i is the capacitance per unit area of the SiO_2 gate dielectric (C_i = 17.7 nF cm^{-2}), V_G is the gate voltage, and V_{th} is the threshold voltage.

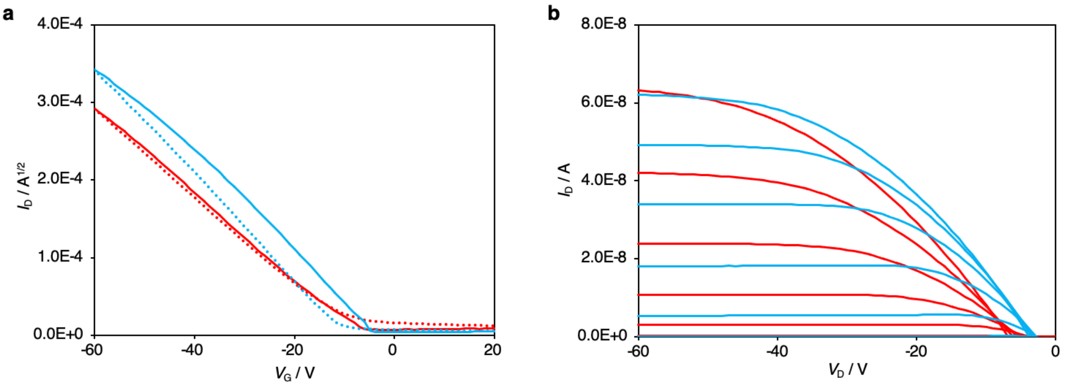

Fig. S3 Transfer (a) and output (b) characteristics of the OFET device for the thin-film layer of compound **1** prepared by vapor deposition on HMDS/PFBT modified (blue) or not modified (red) surface.

5. Computational study

The Gaussian 16 program[S6] running on a NEC LX 110Rh system was used for optimization. Structures were optimized at B3LYP/6-31G(d) with Grimme's D3 type dispersion correction.[S7–S9] Zero-point energy, enthalpy, and Gibbs free energy at 298.15 K and 1 atm were estimated from the gas-phase studies. Harmonic vibration frequency calculation at the same level was performed to verify all stationary points as local minima (with no imaginary frequency) or transition states (with one imaginary frequency). Amsterdam Density Functional (ADF)[S10,S11] calculations were performed using PW91 level of theory[S12] and DZP basis sets. Cartesian coordinates of optimized structures are included in CartesianCoordinates.xyz file.

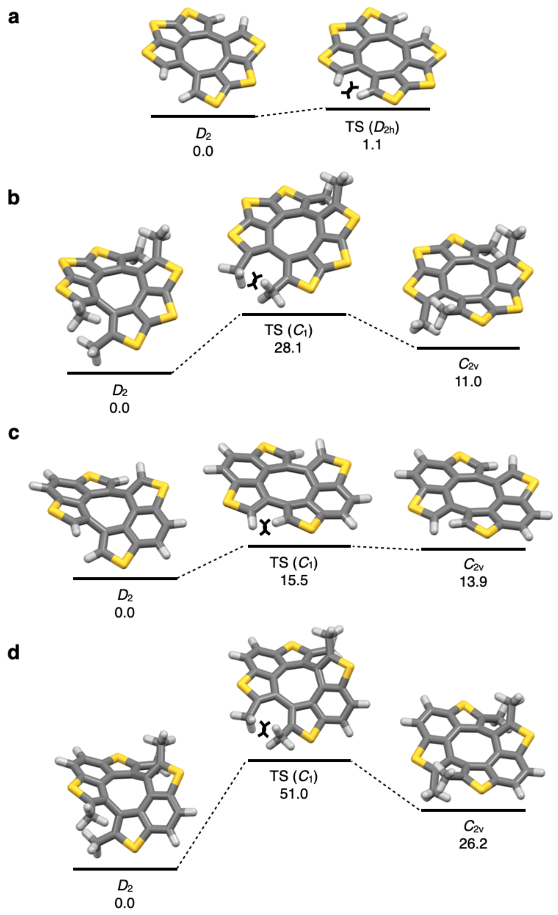

Fig. S4 Local minima and transition states of **4** (a), **1** (b), **7** (c), and **2** (d) with relative Gibbs free energy (kcal·mol^{-1}) calculated using B3LYP-D3 level of theory and 6-31G(d) basis sets.

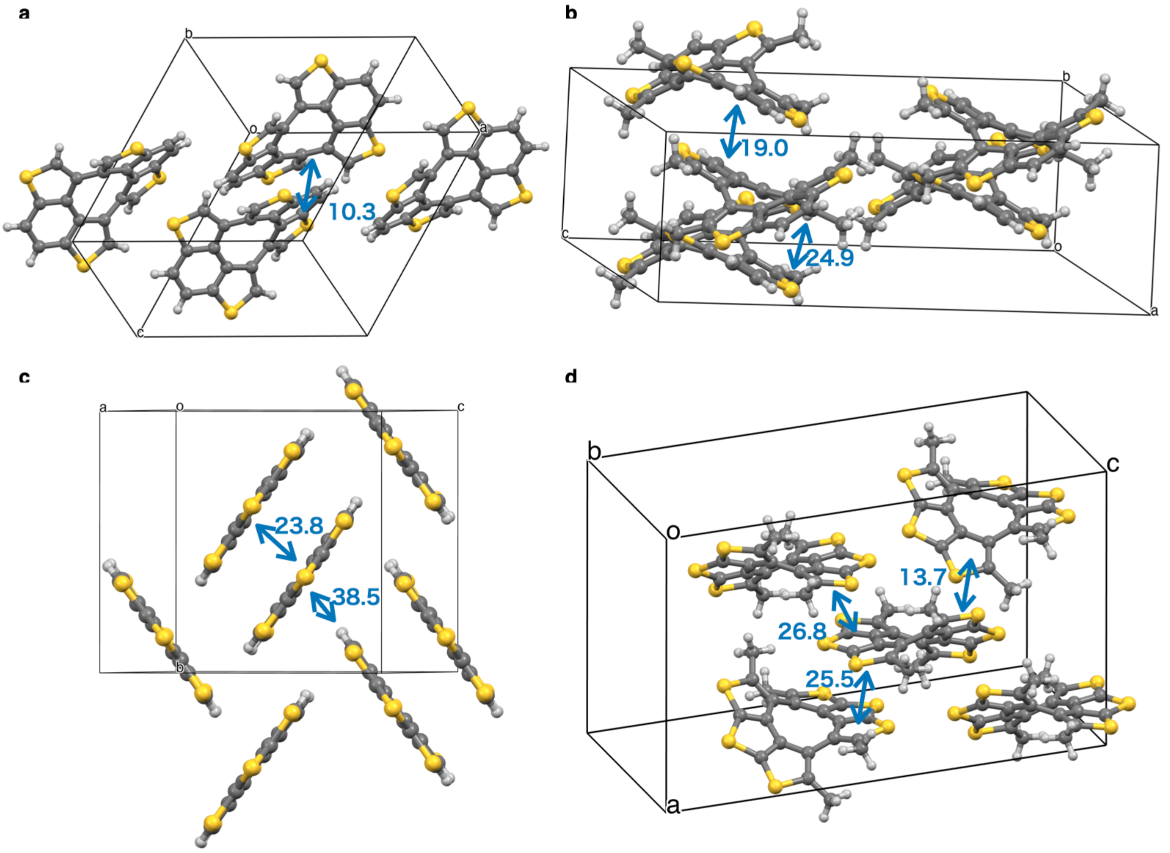

Fig. S5 Representative (>10 meV) transfer integrals (meV) of the crystal structures of **7** (a), **2** (b), **4** (c), and **1** (d) calculated by ADF.

Table S3. Uncorrected and thermal-corrected (298 K) energies of stationary points (Hartree).[a]

	E	*E* + *ZPE*	*H*	*G*
1-D2	-3158.49650161	-3158.234309	-3158.210891	-3158.282962
1-C2v	-3158.47880847	-3158.216659	-3158.193413	-3158.265413
1-TS	-3158.45045971	-3158.188663	-3158.165929	-3158.238167
2-D2	-2517.02320668	-2516.695772	-2516.671654	-2516.744275
2-C2v	-2516.98068190	-2516.653401	-2516.629566	-2516.702595
2-TS	-2516.94015038	-2516.613139	-2516.589813	-2516.663067
4-D2	-3001.22538432	-3001.076426	-3001.058983	-3001.119401
4-TS	-3001.22302398	-3001.074618	-3001.057764	-3001.117683
7-D2	-2359.74037791	-2359.525110	-2359.507474	-2359.568234
7-C2v	-2359.71667564	-2359.501548	-2359.483809	-2359.546007
7-TS	-2359.71660023	-2359.501542	-2359.484677	-2359.543531

[a] *E*: electronic energy; *ZPE*: zero-point energy; *H* (= $E + ZPE + E_{\mathrm{vib}} + E_{\mathrm{rot}} + E_{\mathrm{trans}} + RT$): sum of electronic and thermal enthalpies; *G* (= *H* – *TS*): sum of electronic and thermal free energies.

Table S4. Excitation energies and oscillator strengths (*f*) of **1-D2**, **2-D2**, **4-D2**, and **7-D2** calculated by TD-DFT with B3LYP-D3/6-31G(d) level.

1-D2 (HOMO: 114, LUMO: 115)

S1: 3.9017 eV 317.77 nm f=0.0217
114 ->115 0.69473
S2: 3.9038 eV 317.60 nm f=0.0296
114 ->116 0.69033
S3: 4.0705 eV 304.59 nm f=0.0000
113 ->116 0.59732
114 ->117 -0.35476
S4: 4.0898 eV 303.15 nm f=0.0023
113 ->115 0.66972
113 ->118 -0.11096
114 ->119 0.16884
S5: 4.0922 eV 302.97 nm f=0.0002
112 ->115 0.67975
112 ->118 -0.13987
S6: 4.1104 eV 301.64 nm f=0.0261
112 ->116 0.60846
114 ->118 0.33092
S7: 4.2802 eV 289.67 nm f=0.0819
110 ->120 0.10917
112 ->116 -0.32961
114 ->118 0.59128
S8: 4.3129 eV 287.48 nm f=0.0000
110 ->115 -0.23647
113 ->116 0.34051
114 ->117 0.55375
S9: 4.3652 eV 284.03 nm f=0.0992
113 ->115 -0.16573
114 ->119 0.66352
114 ->122 0.10642
S10: 4.4275 eV 280.03 nm f=0.0203
110 ->116 0.67255
111 ->117 0.10386
112 ->117 -0.11293

2-D2 (HOMO: 112, LUMO: 113)

S1: 3.5802 eV 346.31 nm f=0.1035
111 ->113 -0.20951
112 ->114 0.66972
S2: 3.6475 eV 339.91 nm f=0.0462
111 ->114 -0.16093
112 ->113 0.68224
S3: 3.9098 eV 317.11 nm f=0.0345
111 ->114 0.67816
112 ->113 0.14711
S4: 3.9881 eV 310.88 nm f=0.1066
109 ->114 0.18420
110 ->113 0.65587
111 ->116 -0.12210
112 ->117 -0.11227
S5: 3.9994 eV 310.01 nm f=0.0000
109 ->113 0.20746
110 ->114 0.63391
111 ->117 -0.12383
112 ->116 -0.17098
S6: 4.0223 eV 308.24 nm f=0.2473
111 ->113 0.65717
112 ->114 0.18753
S7: 4.0767 eV 304.13 nm f=0.0278
108 ->113 0.12639
109 ->114 -0.26982
110 ->113 0.12944
112 ->115 0.61822
S8: 4.1893 eV 295.95 nm f=0.0000
108 ->114 -0.10164
109 ->113 0.58625
110 ->114 -0.24317
111 ->115 -0.21943
112 ->116 -0.17782
S9: 4.2404 eV 292.39 nm f=0.0000
109 ->114 0.58251
110 ->113 -0.19216
111 ->116 -0.10273
112 ->115 0.30331
112 ->117 -0.12313
S10: 4.3617 eV 284.26 nm f=0.0000
108 ->114 0.36272
109 ->113 0.24171
111 ->115 0.54031

4-D2 (HOMO: 98, LUMO: 99)

```
S1: 3.8329 eV    323.47 nm    f=0.0161
        95 ->100            -0.10851
        98 -> 99             0.69444
S2: 3.8529 eV    321.80 nm    f=0.0061
        95 -> 99            -0.10353
        98 ->100             0.68951
S3: 4.1442 eV    299.18 nm    f=0.0020
        97 -> 99             0.68205
        97 ->102             0.12484
S4: 4.1766 eV    296.85 nm    f=0.0319
        97 ->100             0.55649
        98 ->102             0.41475
S5: 4.2044 eV    294.89 nm    f=0.0000
        96 ->100             0.41414
        98 ->101             0.56316
S6: 4.3159 eV    287.28 nm    f=0.0000
        96 -> 99             0.67732
        98 ->103            -0.13040
S7: 4.3604 eV    284.34 nm    f=0.1373
        94 ->105            -0.11983
        97 ->100            -0.36204
        98 ->102             0.50778
        98 ->104            -0.29246
S8: 4.4776 eV    276.90 nm    f=0.0000
        94 -> 99             0.20795
        96 ->100             0.54177
        98 ->101            -0.37712
        98 ->105            -0.10088
S9: 4.4949 eV    275.83 nm    f=0.0040
        95 -> 99             0.66733
        97 ->102            -0.17578
S10: 4.5601 eV    271.89 nm    f=0.0296
        95 ->100             0.65973
        98 ->104            -0.19218
```

7-D2 (HOMO: 96, LUMO: 97)

```
S1: 3.6531 eV    339.40 nm    f=0.0319
        96 -> 97             0.69436
S2: 3.7038 eV    334.75 nm    f=0.0886
        94 -> 97             0.18701
        96 -> 98             0.67442
S3: 3.9629 eV    312.87 nm    f=0.0552
        95 -> 97             0.65507
        96 -> 99             0.23353
S4: 4.0862 eV    303.43 nm    f=0.0000
        93 -> 97            -0.12131
        94 ->101             0.11004
        95 -> 98             0.66179
        96 ->100             0.13950
S5: 4.1388 eV    299.57 nm    f=0.1228
        92 -> 97             0.14573
        93 -> 98             0.15451
        95 -> 97            -0.19612
        96 -> 99             0.62799
S6: 4.2186 eV    293.90 nm    f=0.0080
        94 -> 98             0.65923
        95 -> 99            -0.23078
S7: 4.2273 eV    293.29 nm    f=0.1756
        93 ->101             0.10104
        94 -> 97             0.65744
        95 ->100             0.12890
        96 -> 98            -0.15737
S8: 4.3107 eV    287.62 nm    f=0.0000
        93 -> 97             0.57423
        94 -> 99            -0.13637
        95 -> 98             0.17283
        96 ->100            -0.31611
S9: 4.4404 eV    279.22 nm    f=0.0028
        93 -> 98             0.60092
        94 ->100             0.14724
        95 -> 97             0.13755
        96 -> 99            -0.17040
        96 ->101             0.25337
S10: 4.5157 eV    274.56 nm    f=0.0256
        94 -> 98             0.20940
        95 -> 99             0.63883
        95 ->101            -0.14702
```

6. References

[S1] S. Zhang, X. Liu, C. Li, L. Li, J. Song, J. Shi, M. Morton, S. Rajca, A. Rajca and H. Wang, *J. Am. Chem. Soc.*, 2016, **138**, 10002–10010.

[S2] L. Li, S. Zhao, B. Li, L. Xu, C. Li, J. Shi and H. Wang, *Org. Lett.*, 2018, **20**, 2181–2185.

[S3] G. M. Sheldrick, *Acta Crystallogr.,* 2015, **A71**, 3–8.

[S4] G. M. Sheldrick, *Acta Crystallogr.,* 2015, **C71**, 3–8.

[S5] O. V. Dolomanov, L. J. Bourhis, R. J. Gildea, J. A. K. Howard and H. Puschmann, *J. Appl. Crystallogr.,* 2009, **42**, 339–341.

[S6] M. J. Frisch, G. W. Trucks, H. B. Schlegel, G. E. Scuseria, M. A. Robb, J. R. Cheeseman, G. Scalmani, V. Barone, G. A. Petersson, H. Nakatsuji, X. Li, M. Caricato, A. V. Marenich, J. Bloino, B. G. Janesko, R. Gomperts, B. Mennucci, H. P. Hratchian, J. V. Ortiz, A. F. Izmaylov, J. L. Sonnenberg, D. Williams-Young, F. Ding, F. Lipparini, F. Egidi, J. Goings, B. Peng, A. Petrone, T. Henderson, D. Ranasinghe, V. G. Zakrzewski, J. Gao, N. Rega, G. Zheng, W. Liang, M. Hada, M. Ehara, K. Toyota, R. Fukuda, J. Hasegawa, M. Ishida, T. Nakajima, Y. Honda, O. Kitao, H. Nakai, T. Vreven, K. Throssell, J. A. Montgomery, Jr., J. E. Peralta, F. Ogliaro, M. J. Bearpark, J. J. Heyd, E. N. Brothers, K. N. Kudin, V. N. Staroverov, T. A. Keith, R. Kobayashi, J. Normand, K. Raghavachari, A. P. Rendell, J. C. Burant, S. S. Iyengar, J. Tomasi, M. Cossi, J. M. Millam, M. Klene, C. Adamo, R. Cammi, J. W. Ochterski, R. L. Martin, K. Morokuma, O. Farkas, J. B. Foresman and D. J. Fox, Gaussian 16, Revision B.01, Gaussian, Inc., Wallingford CT, 2016.

[S7] A. D. Becke, *J. Chem. Phys.,* 1993, **98**, 5648–5652.

[S8] C. Lee, W. Yang and R. G. Parr, *Phys. Rev. B,* 1988, **37**, 785–789.

[S9] S. Grimme, J. Antony, S. Ehrlich, H. Krieg and J. Chem. Phys. 200, **132**, 154104.

[S10] ADF ADF2022.101 and ADF2023.102, Theoretical Chemistry, Vrije Universiteit, Amsterdam, The Netherlands, http://www.scm.com

[S11] G. te Velde, F. M. Bickelhaupt, E. J. Baerends, C. Fonseca Guerra, S. J. A. van Gisbergen, J. G. Snijders and T. Ziegler, *J. Comput. Chem.,* 2001, **22**, 931–967.

[S12] J. P. Perdew, J. A. Chevary, S. H. Vosko, K. A. Jackson, M. R. Pederson, D. J. Singh and C. Fiolhais, *Phys. Rev. B*, 1992, **46**, 6671–6687.

7. ^{1}H and ^{13}C NMR Spectra of Products

^{1}H NMR spectrum of **1** (400 MHz, $CDCl_3$)

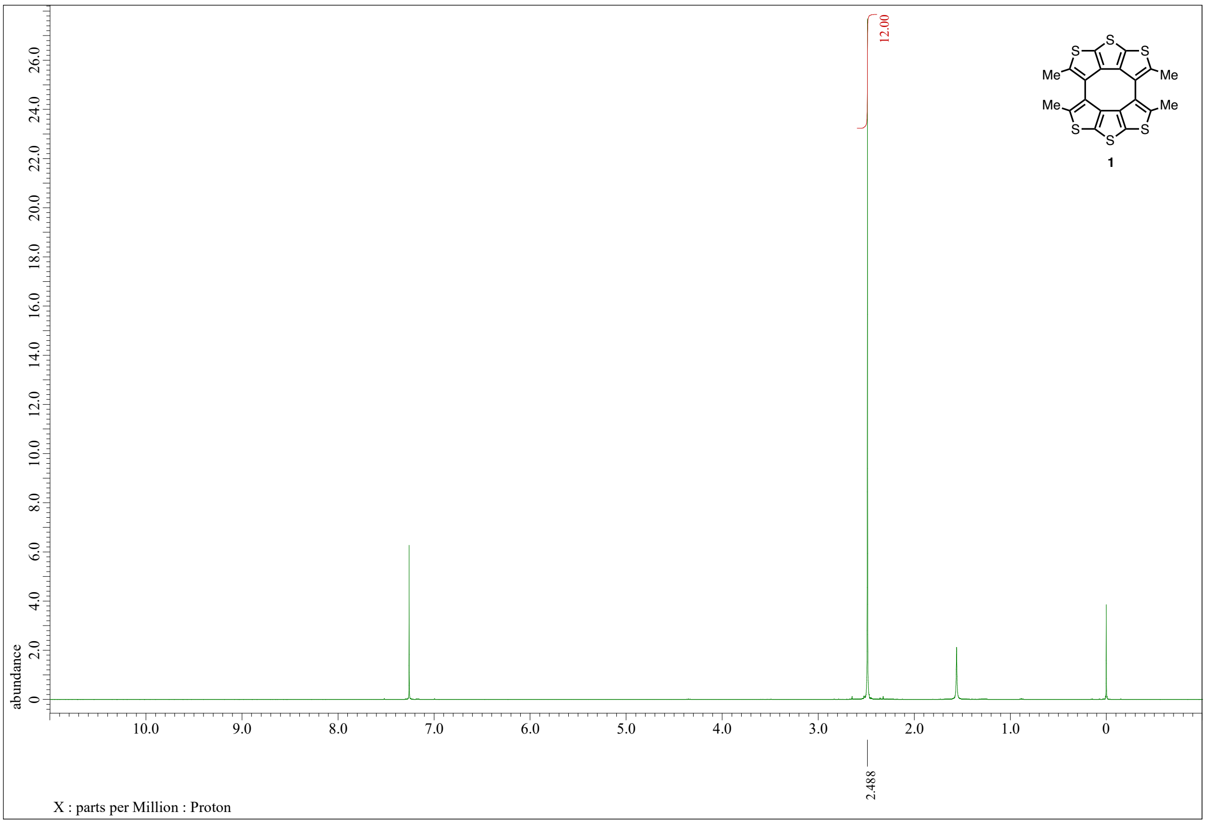

^{13}C NMR spectrum of **1** (100 MHz, $CDCl_3$)

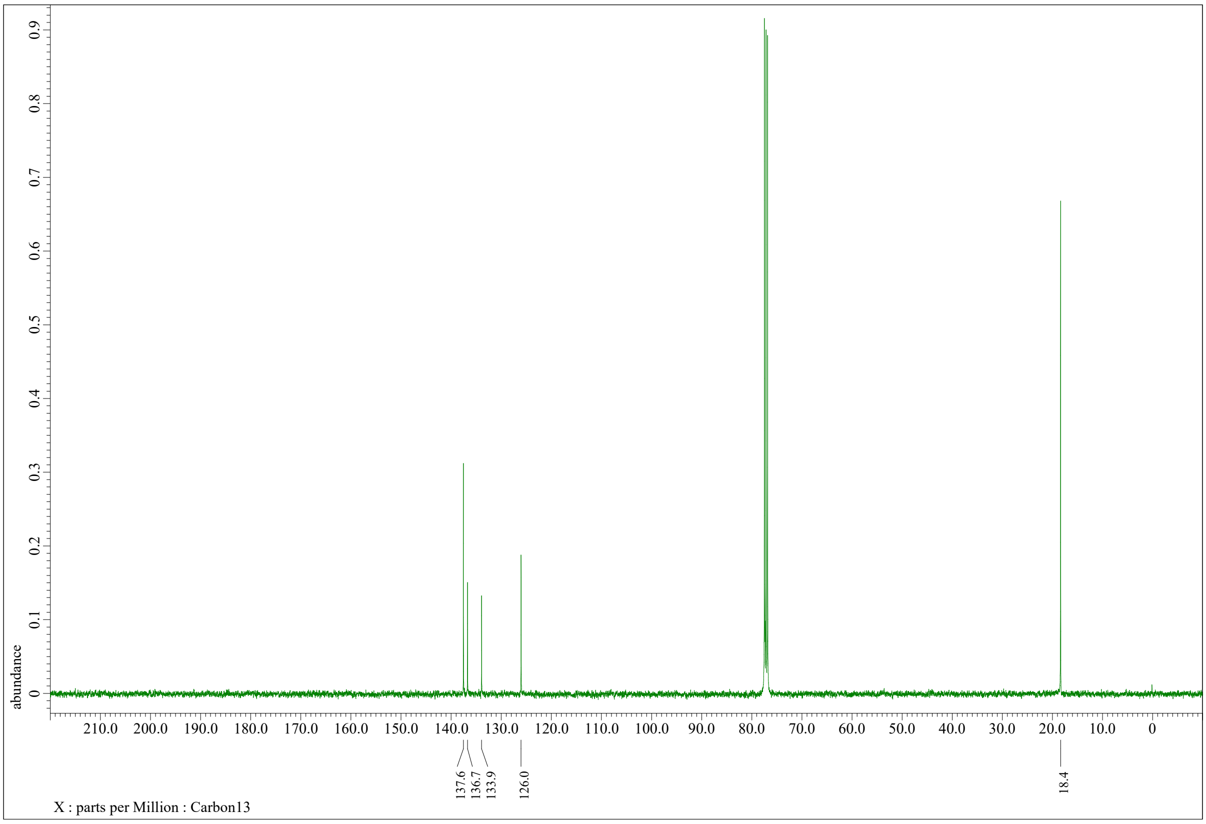

^{1}H NMR spectrum of **5** (400 MHz, $CDCl_3$)

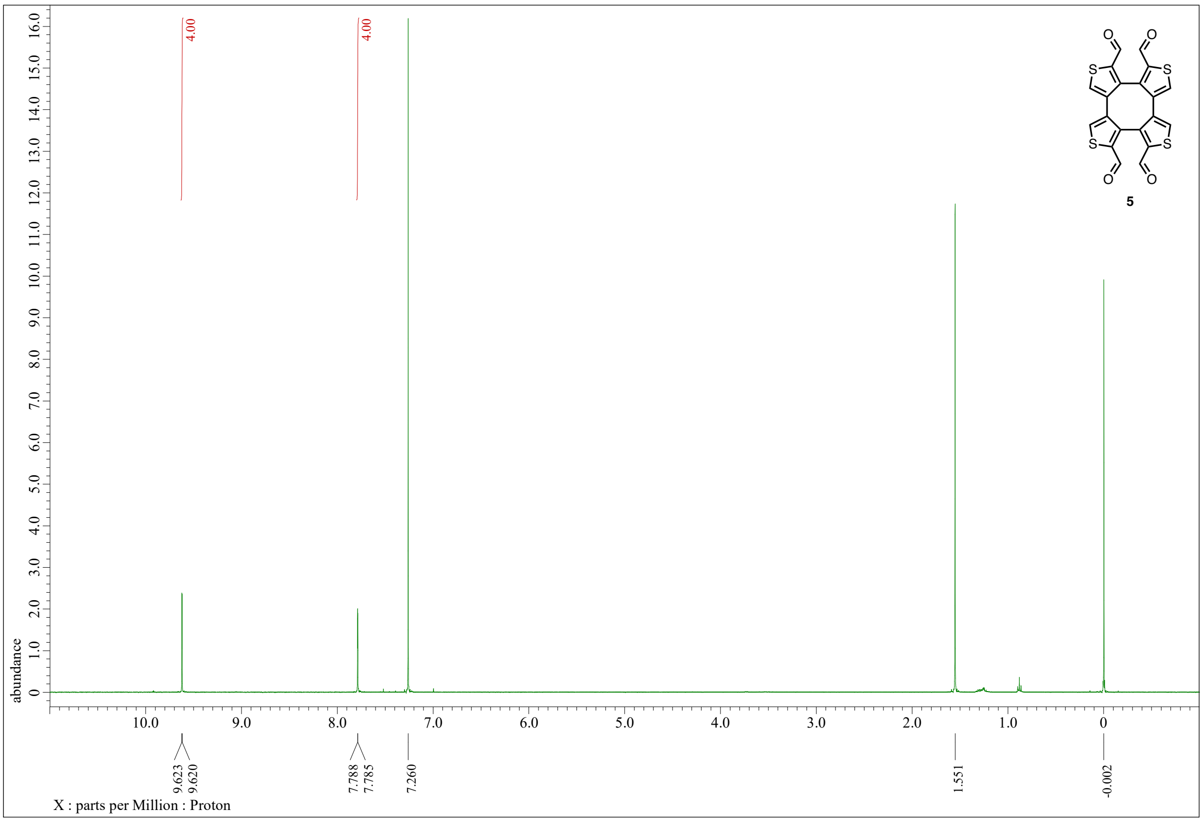

^{13}C NMR spectrum of **5** (100 MHz, $CDCl_3$)

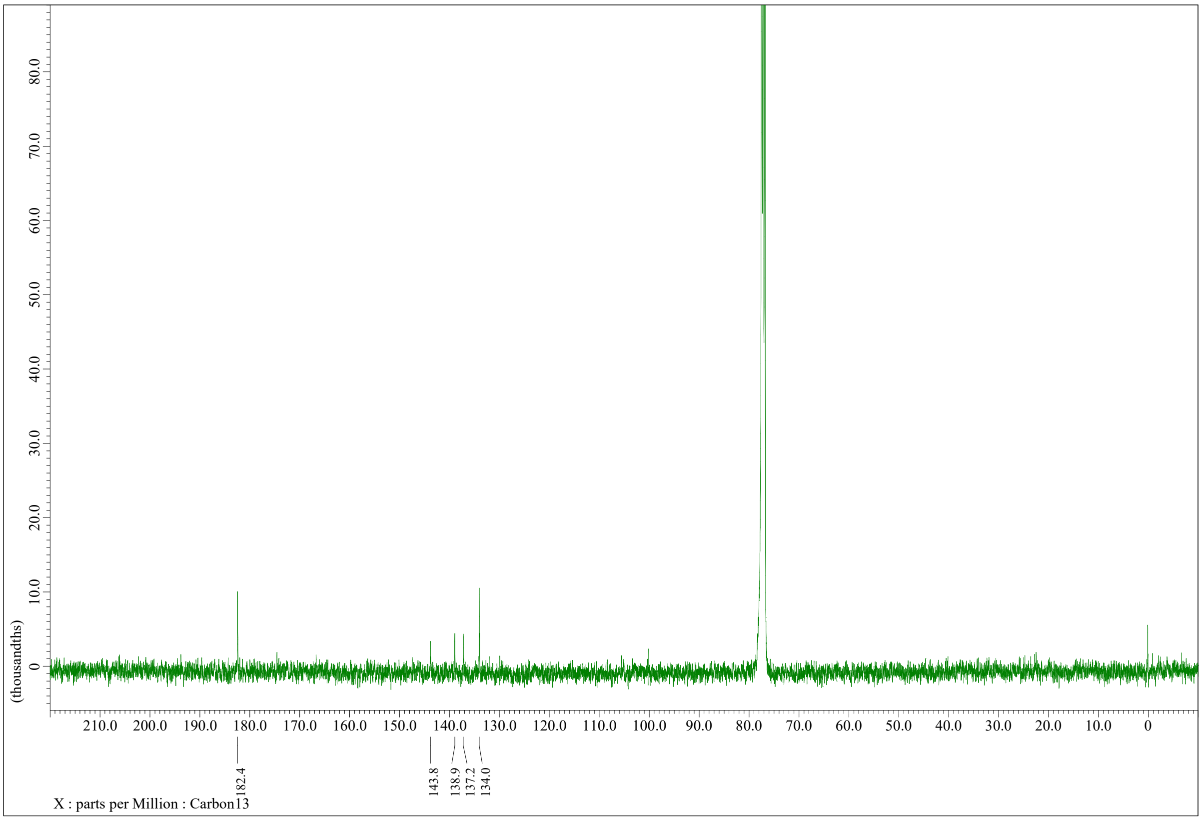

^{1}H NMR spectrum of **6** (400 MHz, CDCl$_3$)

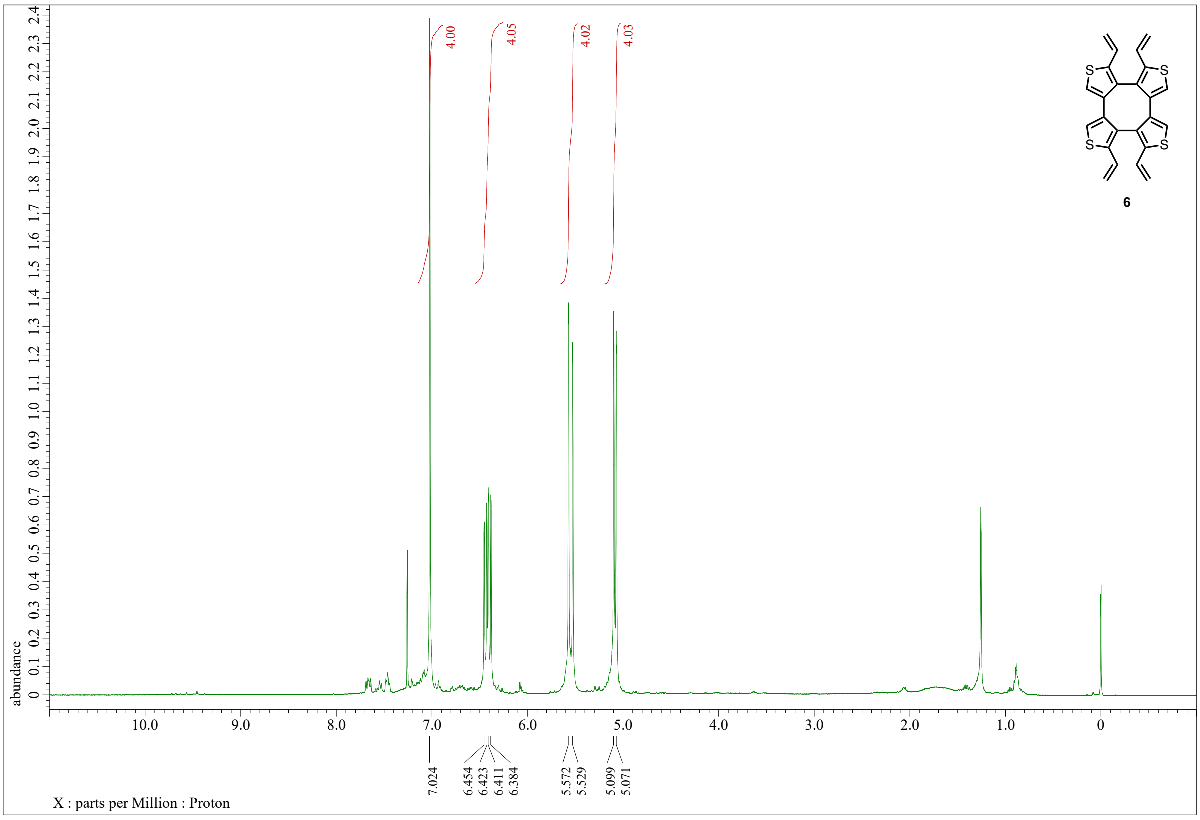

^{13}C NMR spectrum of **6** (100 MHz, CDCl$_3$)

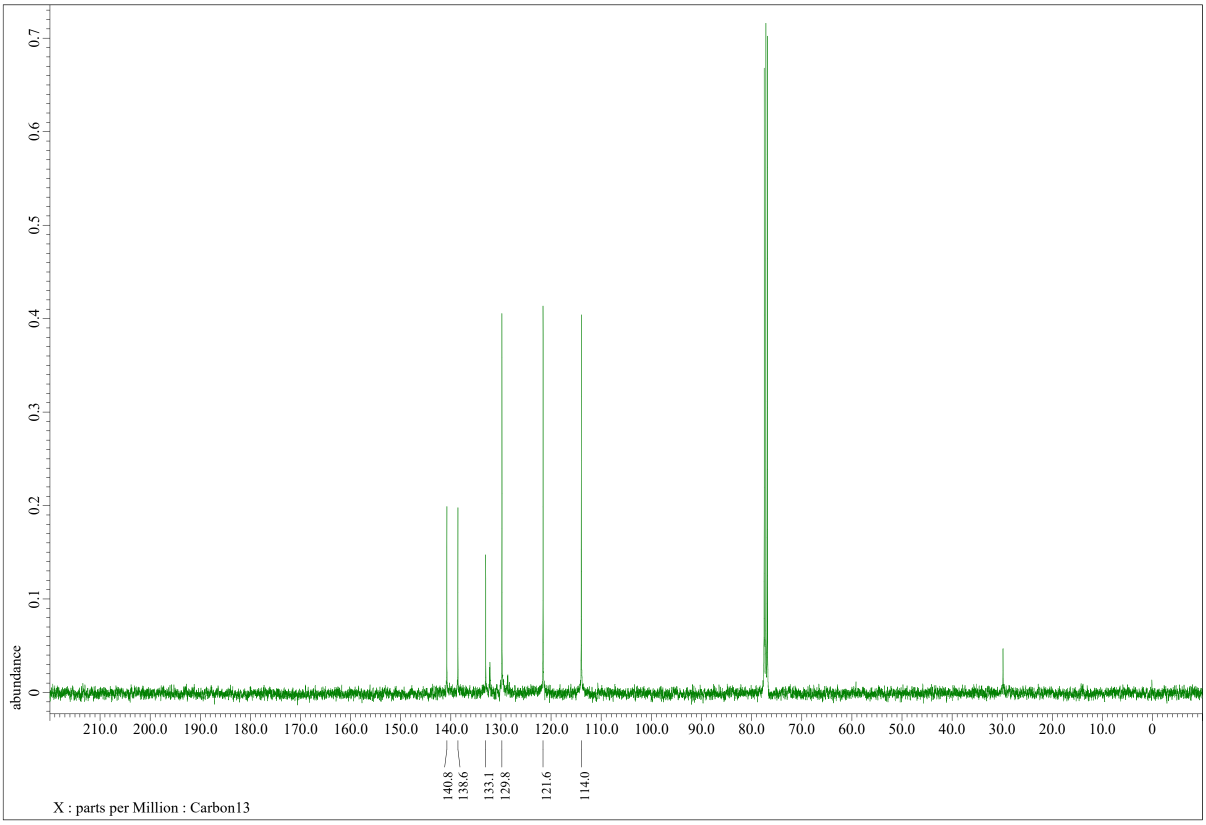

^{1}H NMR spectrum of **7** (400 MHz, CDCl$_3$)

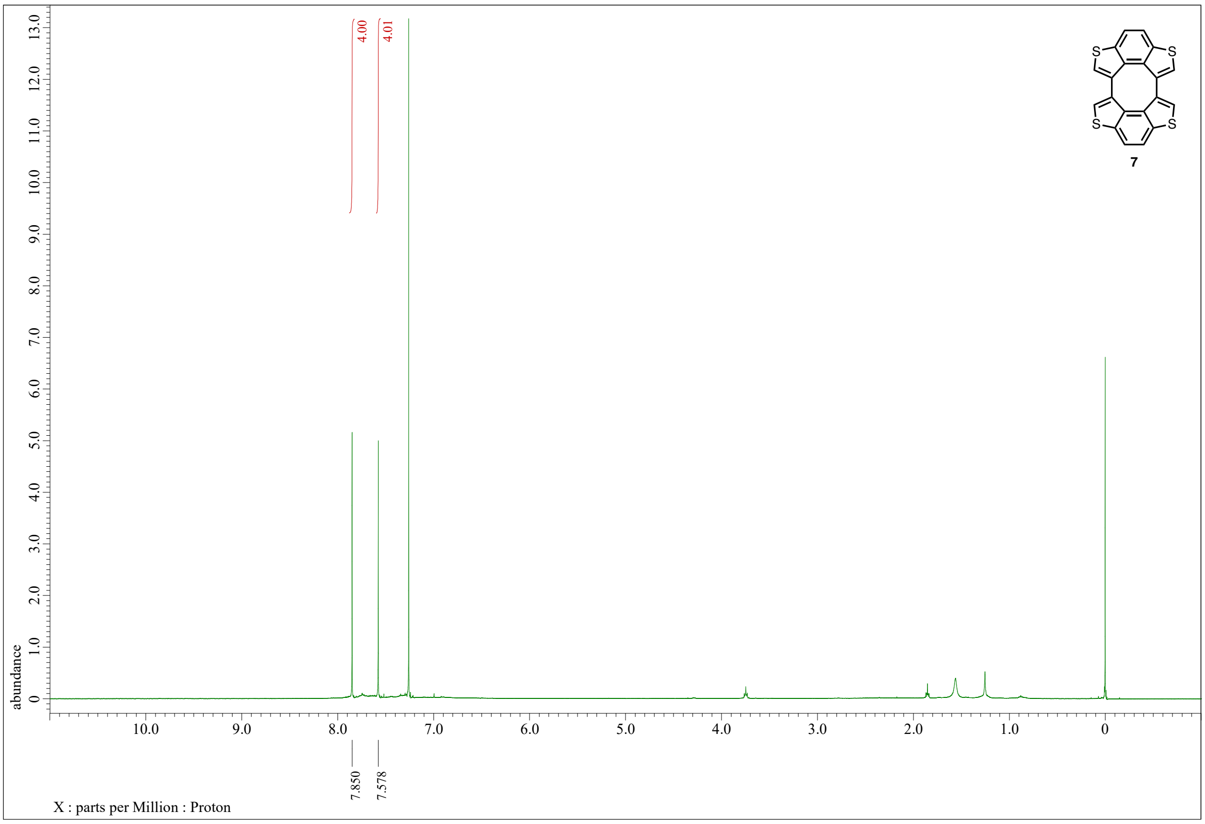

^{13}C NMR spectrum of **7** (100 MHz, CDCl$_3$)

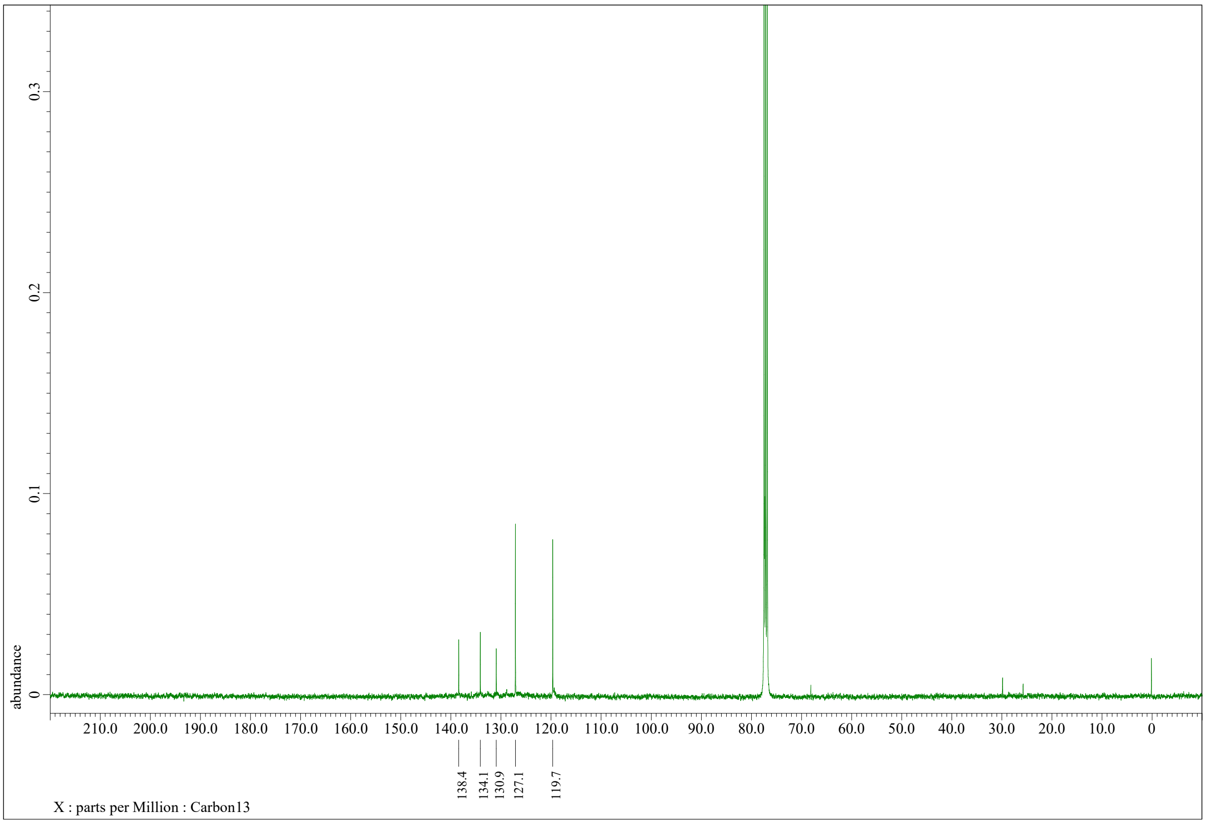

^{1}H NMR spectrum of **2** (400 MHz, CDCl$_3$)

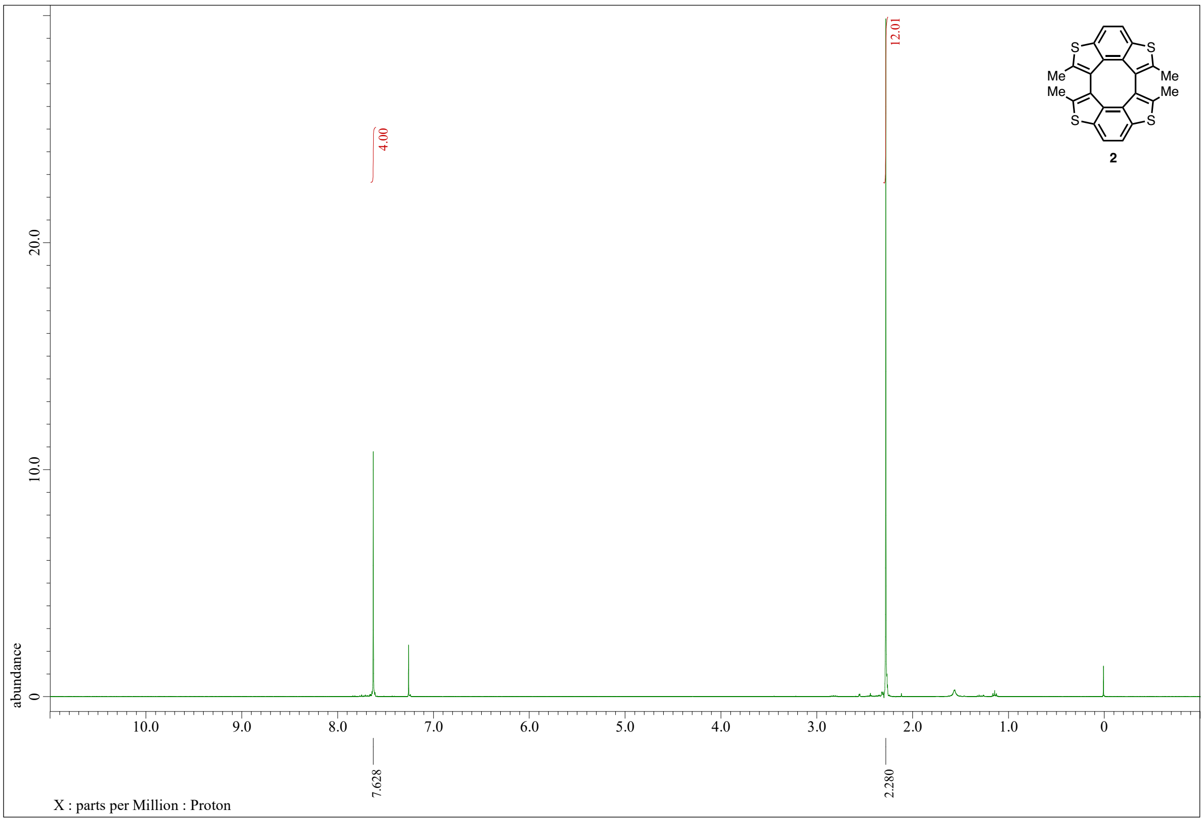

^{13}C NMR spectrum of **2** (100 MHz, CDCl$_3$)